DOI 10.5162/16dss2022/P20

Split-Ring Resonator for measuring low amounts of glutamic acid in pure water

Kirsten Dehning, Alexander Gossmann, Moritz Hitzemann und Stefan Zimmermann

Leibniz University Hannover, Institute of Electrical Engineering and Measurement Technology, Department of Sensors and Measurement Technology, Appelstr. 9A, 30167 Hannover, Germany

Contact: dehning@geml.uni-hannover.de

Introduction

Split-ring resonators (SRR) are electrical circuits that are easy to manufacture and consist of only two microstrip lines patterned on a printed circuit board (PCB) to form a resonator. One of the two microstrip lines is formed to a ring with a split that serves as the sensitive region. The second microstrip line is used to couple an electromagnetic wave into and out of the split-ring structure. The split-ring structure works like a RLC series resonant circuit where the conductor and the polarization loses are the resistor *R*, the ring is the coil *L* and the split is the capacitor *C*, see equation 1 for calculating the resonance frequency $f_{res,e}$ of the resonator [1,2]. Considering additional losses, a shift of this resonance frequency is possible.

$$f_{res,e} = \frac{1}{2\pi\sqrt{LC}} \tag{1}$$

At resonance frequency, the transmission through the first microstrip line reaches a minimum since the electromagnetic wave couples into the split-ring structure. The resonance frequency particularly changes when the permittivity, polarization losses or conductivity of the split capacitor dielectric changes. With the transmission line theory a good estimation of the resulting resonance frequency f_{res} for a given sample at the split capacitor *C* with a given complex permittivity is possible, see equation 2 with l_0 being half of the geometric ring length, v being the propagation velocity and Z_L being the wave impedance of the ring structure [3].

$$f_{res} = \frac{v}{2l_o + \sqrt{4l_o^2 + 16l_o v Z_L \cdot C}} \tag{2}$$

The capacitor in equation 2 also depends on the parasitic capacities between ground and the two microstrip lines C_p and can be assumed following equation 3 with $C_{0,p}$ being the unloaded (air) split capacitance and $\varepsilon'_{r,p}$ being the real part of the relative permittivity of the sample in the split.

$$C = C_P + C_{0,p} \cdot \varepsilon'_{r,p} \tag{3}$$

Therefore, SRRs are very sensitive to changes in the dielectric properties of a sample at the split capacitor that sets the resonant circuit and can be used as sensitive detectors to measure the properties of liquids [4]. For highest sensitivity, the split capacitor needs to be as large as possible in relation to the parasitic capacitances [3]. Therefore, we use an interdigital finger structure to increase the split capacitance.

In addition to the resonance frequency, which is affected by the properties of the split capacitor dielectric and thus the sample at the split capacitor, the attenuation and quality factor, respectively, is also a measure for any sample induced polarization and ohmic losses. Without any liquid sample covering the sensitive region of the SRR, the attenuation mainly depends on the coupling between the two microstrip lines, the losses in the used PCB material (mainly polarization losses), FR4 or Rogers, and on the geometry and material (ohmic losses) of the used microstrip lines. Another effect to be considered is the frequency-dependent skin effect. Due to the skin effect, the ohmic losses in any conductor increase with increasing frequency. At higher frequencies, the conducting cross section of the conductor reduces and the electric current concentrates near the surface. For SRRs, this needs to be considered when the used resonance frequency increases with reduced ring dimensions. For a real measured SRR with an geometric ring length of 48 mm, which corresponds to a SRR resonance frequency of approximate 1.2 GHz (without considering the capacitive extension of the ring length), the skin depth can be calculated with equation 4 with ρ being the resistivity of the conductor, f being the frequency, μ being the permeability of the conductor and ε being the permittivity.

$$\delta = \sqrt{\frac{2\rho}{f\mu}} \sqrt{\sqrt{1 + (\rho f \varepsilon)^2} + \rho f \varepsilon} \tag{4}$$

For metals such as copper and the used frequencies in the GHz range equation 4 simplifies to equation 5. Equation 5 depends on the resistivity of the conductor

ρ the frequency f and the permeability of the conductor μ.

$$\delta = \sqrt{\frac{2\rho}{f\mu}} \tag{5}$$

At a resonance frequency of 1.2 GHz, the skin depth for a full copper conductor is at 1.88 µm, for the normally used PCBs the track thickness of copper is 35 µm. With additional coating e.g. chemical gold, the thickness increases by another 3 µm to 6 µm for the nickel primer and 0.05 µm to 0.1 µm for the gold. With this coating, the current concentrates in the thin gold layer and partly in the nickel layer increasing the overall resistance. Furthermore, the nickel reduces the skin depth due to its high permeability to 0.156 µm so that the current concentrates in a very small cross-section of the conductor (0.05 µm gold plus 0.151 µm nickel). This increases the effective specific resistivity of the track from 25.031 µΩ·mm for DC currents to 62.954 µΩ·mm for 480 MHz and 76.146 µΩ·mm for 1.2 GHz [5]. For lower resonance frequencies, the ring length increases but the skin depth gets higher so a larger cross section of the conductor is used, reducing the resistance.

Methods and Materials

The standard measurement technique for the determination of the SRR properties such as resonance frequency and quality factor is a broadband frequency sweep using a vector network analyzer (VNA). The VNA has the advantage of analyzing the SRR by measuring the transmitted and reflected signals at the inputs and outputs of the SRR. These measurements are performed at several discrete frequencies in the frequency range of the SRR.

SRRs can have many different topologies. They can be round [1], quadratic [3] or rectangular [2]. However, the form of the split has the greatest variance in literature. From the simplest form of a split [2] to a tapered split [6], an extended split [7] and interdigital structures [3], there are many different topologies.

In this work, we use three different quadratic SRR topologies with cut-off edges, different ring lengths and thus different resonance frequencies in the unloaded state (in air). All used SRRs are made of FR4 with 1.4 mm thickness and a gold plated copper layer with 38.05 µm to 41.1 µm thickness depending on the thickness of the coating. On the top side (shown in Fig. 1), the two described microstrip lines are patterned. The bottom side contains the ground plane. In order to prevent the electric field from appearing between the split capacitor and the ground plane the ground plane has been removed directly opposite the split capacitor. This is necessary to increase the electric field above the split capacitor so that the electric field penetrates the sample. The top of the SRR, except for the copper surfaces, are coated with solder mask with a thickness of about 25 µm to prevent liquid samples from penetrating the PCB substrate. For highest sensitivity, the split capacitor area is increased by an interdigital finger structure [3].

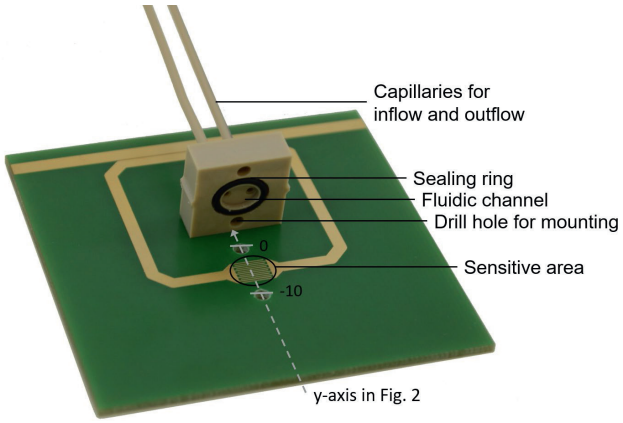

Fig. 1: Split-ring resonator #1 with the lid open (for better visualization), which contains the fluidic connection components.

SRR #1 (Fig. 1) has an length of edge of 32 mm and 6 fingers with a length of 5 mm, a width of 150 µm and a spacing of 150 µm. SRR #2 has an length of edge of 16 mm and 5 fingers with a length of 5 mm, a width of 200 µm and a spacing of 200 µm. SRR #3 has an length of edge of 14 mm and 4 fingers with a length of 4 mm, a width of 500 µm and a spacing of 500 µm. Capillary fluidic interconnects are provided by a lid made of polyetheretherketone. The lid is screwed to the PCB covering the split capacitor and sealed with a sealing ring.

Electromagnetic simulations performed in CST Microwave Studio® show that the electric field strength of the three SRRs is between 100 kV/mm and 200 kV/mm in the plane of the split capacitors. This is illustrated in Fig. 2 for SRR #1. The y-position is directed from the lower edge of the PCB over the capacitor, the ring and the second microstrip line up to the upper edge, see Fig. 1. The position of the capacitor is between -7 mm and -1 mm. The position of the gap between the two microstrip lines is at 25 mm therefore an electric field can also be determined at that position. As seen from Fig. 2, only 500 µm above the plane of the split capacitor the field strength drops by a factor of about 10. Thus, the part of a sample that is above 500 µm does not significantly affect the resonance frequency. Therefore, the lid has a cavity of

just 800 µm and thus properly covers the sensitive area of the SRR.

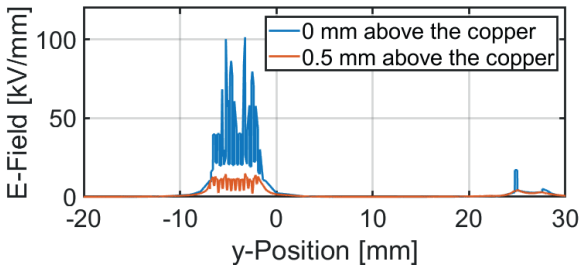

Fig. 2: Electric field of SRR #1 in the plane of the split capacitor and 500 µm above simulated in CST Microwave Studio®. The position of the capacitor in y-direction (see Fig. 1) is between -7 mm and -1 mm.

Results

The three SRRs are compared by measuring different amounts of glutamic acid in pure water (UHPLC-MS grade, *Sigma-Aldrich*). The resonance frequency f_{res}, the quality factor Q and the attenuation at resonance frequency were determined using a vector network analyzer. If not otherwise state, the measurement settings were as follows: The frequency steps are set to 50 kHz, the bandwidth is 100 Hz and the power 0 dBm. Thus, a measurement time of 83 s results for a frequency range of 500 MHz. The frequency range is set specifically for each SRR (50 MHz to 550 MHz for SRR #1, 100 MHz to 600 MHz for SRR #2 and 250 MHz to 750 MHz for SRR #3). The S_{21}-parameter over frequency for the three SRRs with different concentrations of glutamic acid in pure water is shown in Fig. 3.

The resonance frequency of SRR #1 does not differ significantly. It ranges from 210.8 MHz for pure water to 210.3 MHz for 4 g/l glutamic acid in pure water. The quality factor decreases from 35.73 for pure water to 18.45 for 4 g/l glutamic acid in pure water. Furthermore, the maximum attenuation of SRR #1 also decreases with increasing concentration of glutamic acid from -1.63 dB to -0.89 dB. For SRR #2, the resonance frequency decreases with increasing concentration from 316.3 MHz for pure water to 314.2 MHz for 4 g/l glutamic acid in pure water. The quality factor decreases with increasing concentration from 33.29 to 18.48. The attenuation also decreases with increasing concentration of glutamic acid from -1.05 dB to -0.65 dB. With increasing concentration of glutamic acid in pure water, the resonance frequency of SRR #3 decreases from 465.1 MHz to 462.8 MHz. The quality factor decreases from 27.04 to 17.94. Finally, the attenuation decreases with increasing concentration of glutamic acid from -1.23 dB to -0.91 dB. The above results are summarized in Table 1. Interestingly, glutamic acid appears to have almost no influence on the resonance frequency. The main effect is a decrease in the attenuation with an increase in the concentration of glutamic acid. Thus, glutamic acid increases the dielectric losses (polarization and ohmic losses) rather than changing permittivity. From the literature it is known that glutamic acid significantly increases the electrical conductivity of pure water from $5.5 \cdot 10^{-5}$ S/m for pure water to $0.34 \cdot 10^{-3}$ S/m for a concentration of 3 mmol/l or 0.5 g/l, and thus to 0.116 S/m for a concentration of 27 mmol/l or 4 g/l glutamic acid in pure water [8].

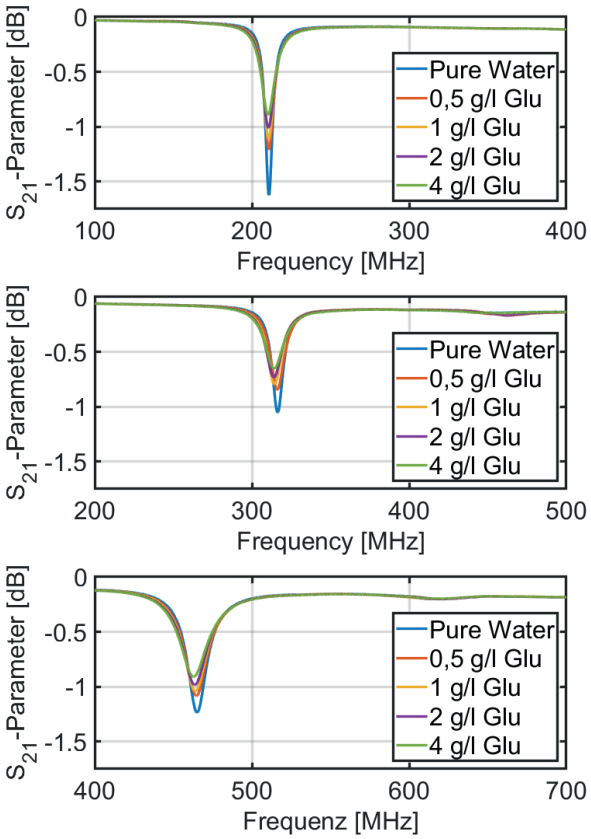

Fig. 3: S_{21}-parameter over frequency for different concentrations of glutamic acid (Glu) in pure water with the three different SRR (SRR #1 (top), SRR #2 (center), SRR #3 (bottom)).

Since the three used SRR have different resonance frequencies and different levels of attenuation, the comparison of the performance of the three SRR with different concentrations of glutamic acid uses the attenuation at a SRR specific frequency rather than the full frequency sweeps. Here, we use the respective resonance frequency that results for pure water at the split. The attenuation at this frequency for the different

SRRs and concentrations of glutamic acid in pure water are plotted in Fig. 4.

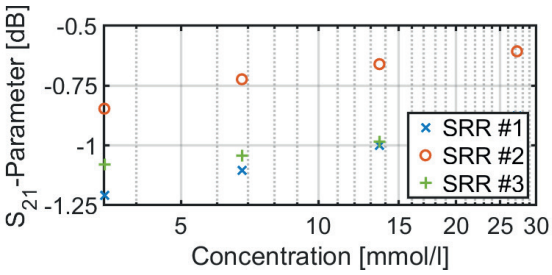

Fig. 4: Comparison of the three SRRs loaded with glutamic acid in pure water, S_{21}-parameters at fixed frequency (resonance frequency when loaded with pure water) plotted against the concentration of glutamic acid.

The sensitivity δS_{21} for glutamic acid in pure water is 0.115 dB/(mmol/l) for SRR #1, 0.044 dB/(mmol/l) SRR #2 and 0.023 dB/(mmol/l) for SRR #3. Considering the noise σ_n the limits of detection (LOD) are calculated. The noise differs between the three SRR. It was determined from 30 measurements. No averaging was possible because of the long measurement time using a VNA. For SRR #1 the standard deviation is 0.0040 dB, for SRR #2 it is 0.0111 dB and for SRR #3 it is 0.0059 dB. Therefore, the limit of detection for glutamic acid in pure water is 105 µmol/l for SRR #1 at $f_{res,1}$ = 211 MHz, 751 µmol/l SRR #2 at $f_{res,2}$ = 316 MHz and 765 µmol/l SRR #3 at $f_{res,3}$ = 465 MHz.

Table 1: Summary of the results with the three different SRR measuring glutamic acid in pure water (glu4 refers to 4 g/l glutamic acid in pure water).

SRR	#1	#2	#3
$f_{res,water}$ [MHz]	210.3	316.3	465.1
$f_{res,glu4}$ [MHz]	210.8	314.2	462.8
Q_{water}	35.73	33.29	27.04
Q_{glu4}	18.45	18.48	17.94
$S_{21,water}$ [dB]	-1.63	-1.05	-1.23
$S_{21,glu4}$ [dB]	-0.89	-0.65	-0.91
δS_{21} [dB/(mmol/l)]	0.115	0.044	0.023
σ_n [dB]	0.0040	0.0111	0.0059
LOD [µmol/l]	105	751	765

Conclusion

Comparing the three SRR quality factors when loaded with pure water, SRR #1 with the lowest resonance frequency has the highest quality factor with 35.73, while SRR #3 has the lowest quality factor with 27.04 at the highest resonance frequency. This can be explained by the skin effect increasing the ohmic losses with increasing frequency rather than decreasing the ohmic losses due to a decreasing length of the ring with increasing frequency. Additional to the highest quality factor SRR #1 has the lowest limit of detection of 105 µmol/l. Furthermore, it has the lowest resonance frequency, which reduces complexity of future measurement electronics for continuous recording of the resonance frequency and attenuation, see Lippmann et al. at Dresdner Sensor-Symposium 2022. Therefore, SRR #1 is best suited for the selected application.

References

[1] A. Verma, S. Bhushan, P. N. Tripathi, M. Goswami, B. R. Singh, A defected ground split ring resonator for an ultra-fast, selective sensing of glucose content in blood plasma, *Journal of Electromagnetic Waves and Applications* 31, 1049–1061 (2017); doi: 10.1080/09205071.2017.1325011.

[2] W. Withayachumnankul, K. Jaruwongrungsee, A. Tuantranont, C. Fumeaux, D. Abbott, Metamaterial-based microfluidic sensor for dielectric characterization, *Sensors and Actuators A: Physical* 189, 233–237 (2013); doi: 10.1016/j.sna.2012.10.027.

[3] T. Reinecke, J.-G. Walter, T. Kobelt, A. Ahrens, T. Scheper, S. Zimmermann, Design and evaluation of split-ring resonators for aptamer-based biosensors, *Journal of Sensors and Sensor Systems* 7, 101–111 (2018); doi: 10.5194/jsss-7-101-2018.

[4] M. Hitzemann, K. J. Dehning, A. V. Gehl, E.-F. Sterr, S. Zimmermann, Fast Readout of Split-Ring Resonators Made Simple and Low-Cost for Application in HPLC, *Electronics* 11, 1139 (2022); doi: 10.3390/electronics11071139.

[5] D. R. Lide, *CRC handbook of chemistry and physics: A ready-reference book of chemical and physical data*. CRC Press, Boca Raton, FLa.; 2009.

[6] W. Withayachumnankul, K. Jaruwongrungsee, C. Fumeaux, D. Abbott, Metamaterial-Inspired Multichannel Thin-Film Sensor, *IEEE Sensors Journal* 12, 1455–1458 (2012); doi: 10.1109/JSEN.2011.2173762.

[7] M. Puentes, C. Weiß, M. Schüßler, R. Jakoby, Sensor Array Based on Split Ring Resonators for Analysis of Organic Tissues, *IEEE MTT-S International Microwave Symposium*, 1–4 (2011); doi: 10.1109/MWSYM.2011.5972633.

[8] A. Apelblat, E. Manzurola, Z. Orekhova, Electrical Conductance Studies in Aqueous Solutions with Glutamic Ions, *Journal of Solution Chemistry* 36, 891–900 (2007); doi: 10.1007/s10953-007-9156-z.